Available online at www.sciencedirect.com
SCIENCE DIRECT
Polymer 46 (2005) 12240–12246
polymer
www.elsevier.com/locate/polymer

Application of an extended Tool–Narayanaswamy–Moynihan model. Part 2. Frequency and cooling rate dependence of glass transition from temperature modulated DSC

Stefan Weyer, Heiko Huth, Christoph Schick *

Institut für Physik, Universität Rostock, 18051 Rostock, Germany

Received 6 March 2005; received in revised form 16 September 2005; accepted 20 October 2005
Available online 10 November 2005

Abstract

In the first part of this paper a Tool–Narayanaswamy–Moynihan-model (TNM) extended by non-Arrhenius temperature dependence of the relaxation time was applied to describe results from temperature modulated DSC (TMDSC). The model is capable to describe the features of the heat capacities measured in TMDSC scan experiments in the glass transition region of polystyrene (PS). In this part the model is applied to bisphenol A-polycarbonate (PC). Both aspects of glass transition, vitrification as well as the dynamic glass transition are again well described by the model. The dynamic glass transition above T_g can be considered as a process in thermodynamic equilibrium. The non-linearity parameter (x) of the TNM model is not needed to describe complex heat capacity as long as the dynamic glass transition is well separated from vitrification. Under such conditions the relation between cooling rate (q_0), and the corresponding frequency (ω) can be found from the two independently observed glass transitions. Fictive temperature and the maximum of the imaginary part of complex heat capacity are used for comparison here. The measurement as well as the TNM-model confirm the relation derived from Donth's fluctuation approach to glass transition, $\omega = q_0/a\delta T$, where $a = 5.5 \pm 0.1$ (confirmed previously experimentally as 6 ± 3) and δT is mean temperature fluctuation of the cooperatively rearranging regions (CRRs).

Keywords: Glass transition; Temperature modulated DSC (TMDSC); Tool–Narayanaswamy–Moynihan model (TNM)

1. Introduction

We consider two aspects of glass transition—(i) the thermal glass transition describing the transition from a super-cooled liquid into a glassy non-equilibrium solid (vitrification) and (ii) the dynamic glass transition a relaxation process in thermal equilibrium (α-relaxation). With temperature-modulated DSC (TMDSC) both aspects of glass transition can be observed simultaneously, thermal glass transition due to underlying cooling and dynamic glass-transition in response to the temperature modulation (frequency dependent). Several models were developed to describe the non-linearity and non-exponentiality of the relaxation behavior at the glass transition [1–14]. The Tool–Narayanaswamy–Moynihan-model (TNM) is known as one powerful tool to describe the measured heat capacity on vitrification and devitrification under a wide variety of experimental conditions and thermal histories, see e.g. Refs. [1–3,15–17] and references therein. In order to improve the predictive power of the models several modifications are described, see e.g. Refs. [9,10,18,19] and references therein. Attempts can be found in literature to describe complex heat capacity by means of the TNM-model too [20–32]. In the first part of this paper [33] we presented a detailed comparison of experimental TMDSC data on polystyrene (PS) with model calculations based on a TNM-model considering a non-Arrhenius (Vogel–Fulcher–Tamann–Hesse (VFTH)) temperature dependence of the equilibrium relaxation time [34–36]. The model does not only describe the typical features of vitrification (cooling rate dependence, curve shape, etc.) and dynamic glass transition (frequency dependence, curve shape of complex heat capacity, etc.). Furthermore it is capable to describe the influence of scanning conditions on the observed complex heat capacity in case both processes are overlapping. A significant dependence of the phase lag or the imaginary part of complex heat capacity on scanning conditions was observed and will be discussed in more detail in the third part of this paper.

* Corresponding author. Tel: +49 381 498 6880; fax: +49 381 498 6882.
E-mail address: christoph.schick@uni-rostock.de (C. Schick).

0032-3861/$ - see front matter © 2005 Elsevier Ltd. All rights reserved.
doi:10.1016/j.polymer.2005.10.097

The influence of partial vitrification on the dynamic glass transition as well as the approach towards equilibrium was observed too. Before discussing these effects in the next parts of this paper we first checked the applicability of the extended TNM model for TMDSC measurements for another polymer, namely bisphenol A-polycarbonate (PC). PC was chosen because of the large number of TMDSC studies [37] and modeling work, e.g. Refs. [1,23,24], already done. In addition we focus on two more questions: (i) Are we able to describe complex heat capacity (dynamic glass transition) as a process in equilibrium by means of the TNM model? Contrary to Ref. [24] we assume that in the course of the temperature oscillation the system does not fall out of equilibrium and therefore T_f always equals T ($x=1$) at temperatures above vitrification. (ii) Another reason for choosing PC was a still unresolved discrepancy between our and Hutchinson et al. data [23] regarding the relationship between cooling rate and the corresponding frequency needed to include T_g values from scanning experiments in Arrhenius plots.

TMDSC allows the simultaneous investigation of vitrification in response to the underlying cooling and the dynamic glass transition in response to the periodic temperature perturbation. From the two independently observed glass transitions the relation between cooling rate and the corresponding frequency can be found [38–40]. From the fluctuation approach to glass transition the following relation was derived [41,42]

$$\omega = \frac{q_o}{a\,\delta T} \tag{1}$$

where δT is mean temperature fluctuation and a equals 5.5 ± 0.1 [42]. This value for a was verified experimentally for a large number of glass forming liquids [39,40]. Nevertheless, different values for $a\,\delta T$ were obtained for the same materials by different authors. See for example Hensel et al. [39] who got $a\,\delta T = 20$ for PS while Hutchinson et al. [23,37] got $a\,\delta T = 5$. It is one of the aims of this study to clarify the reason for this discrepancy by measuring the same PC sample[1] as used by Hutchinson et al. [23] and to model the cooling rate as well as the frequency dependency by means of the extended TNM-model.

2. Experimental

2.1. Calorimetric measurements

The technique of TMDSC and the necessary data treatments are described elsewhere [43–48]. The Lexan 104R bisphenol A-polycarbonate (PC) was from General Electric ($\rho = 1.2$ g/cm^3; $M_W = 28{,}000$ g/mol). DSC measurements were performed to determine conventional or $C_{p\,total}$ and TMDSC to determine complex heat capacity. A computer controlled Perkin–Elmer Instruments DSC2 and a Setaram DSC121 were used for the TMDSC and DSC measurements. The sample mass was $m_{PC} = 13$ mg and $m_{PC} = 240$ mg for the DSC2 and the DSC121, respectively. The temperature scale of the calorimeters was calibrated in DSC mode at zero heating rate by indium and lead according to the recommendations of GEFTA [49], and was checked in TMDSC mode by the smectic-to-nematic transition of 8OCB [50,51]. The determination of complex heat capacity, especially the correction of the measured phase angle for contributions originating from heat transfer, was performed as described in [52]. All TMDSC experiments if not stated otherwise were carried out with sinusoidal temperature modulation with amplitude $A_T = 0.5$ K and modulation period $t_p = 60$ s. The underlying cooling rate was varied between $q_0 = -1$ K/min and $q_0 = -0.001$ K/min.

2.2. Definition of experimental conditions

TMDSC obtains information from the response of the sample on two independent perturbations simultaneously. These are the thermal glass transition (vitrification) due to underlying cooling rate and the dynamic glass transition (α-relaxation) due to temperature modulation (frequency dependent). For TMDSC measurements at glass transition one has to consider that vitrification of the sample during the dynamic measurement may interfere with the measured complex heat capacity [23,26,29,31,33]. The interference arises because measurements are performed at low frequencies (mHz) and cooling is relatively fast (K/min). Thermal and dynamic glass transitions are therefore often not well separated in TMDSC measurements. In order to investigate possible interferences we have fixed the dynamic glass transition temperature by using a fixed frequency $f = 0.017$ Hz (period $t_p = 60$ s). Vitrification was shifted in temperature by varying the underlying cooling rate in the range from 1 to 0.001 K/min.

2.3. Tool–Narayanaswamy–Moynihan-model calculations

An extended TNM-model, discussed in detail by Donth et al. [36], was used to describe vitrification and dynamic glass transition as well as possible interferences [33]. In order to obtain complex heat capacity from the extended TNM-model we calculated the heat flow rate from fictive temperature according the temperature–time profile used for the TMDSC measurements. The resulting heat flow rate was Fourier transformed as common in TMDSC. To avoid falsification due to a limited number of points per period we used at least 30 points per period. For slow cooling rates this yields a dramatic increase of the total number of points and consequently in computation time, for details see Refs. [33,53].

The parameters τ_0, $\Delta h^*/R$ and T_∞ of the TNM-model are directly connected with the parameters of the VFTH-equation

$$\log \omega = A + \frac{B}{T - T_\infty} = \frac{1}{2.3026}\left\{-\ln \tau_0 + \frac{-\Delta h^*}{R \times (T - T_\infty)}\right\}, \tag{2}$$

[1] We acknowledge the support by J.M. Hutchinson, Aberdeen, UK, for providing us with the PC sample used in his study.

describing the temperature dependence of the mean relaxation time in equilibrium. They are independently available from heat capacity spectroscopy, see below. It is the idea of the present model to obtain these parameters from independent experiments and not from a fitting of the model to the measured heat capacity curves. Only the remaining two parameters, Kohlrausch exponent β and non-linearity parameter x, were determined by a fitting procedure. This way, most parameters of the TNM model were independently determined from different experiments. The data treatment algorithm is described in the first part of this paper [33].

3. Results

3.1. Determination of the model parameters

First, to confirm the capability of the TNM-model to describe the experimental curves for total as well as complex heat capacity in the glass transition range for other polymers than polystyrene we performed a similar comparison for bisphenol A-polycarbonate. To determine the parameters τ_0, $\Delta h^*/R$ and T_∞ of the TNM-model dynamic calorimetric glass transition temperatures from the so called 3ω-method [54] and TMDSC measurements were fitted to the VFTH function (2), see Fig. 1. This figure includes additionally the results of frequency dependent dielectric and shear compliance measurements. Note that the difference between the curves from heat capacity and dielectric spectroscopy of more than one order of magnitude was not observed for polystyrene and some other polymers [33]. The reason for this vertical shift is not yet understood but it is observed for other polymers too [55].

From the VFTH-fit to the 3ω-method and TMDSC data of Fig. 1 the parameters, $\ln(\tau_0/s) = -31.12$, $\Delta h^*/R = 1580$ K, $T_\infty = 370$ K, were determined. The remaining parameters, β and x, were obtained from the standard DSC measurements on heating and cooling at 1 K/min as described in [33]. A fit was

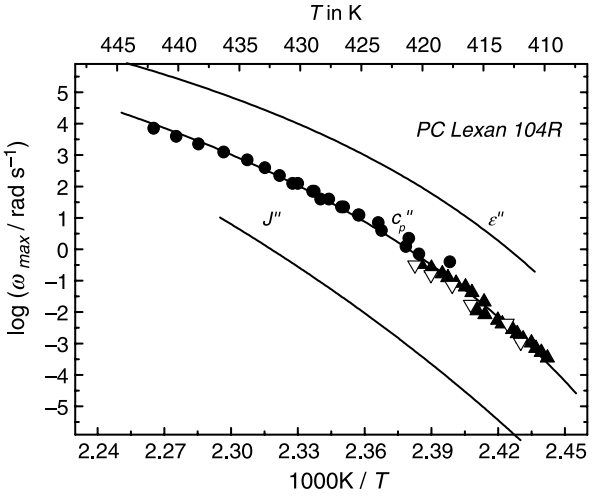

Fig. 1. Activation diagram of bisphenol A-polycarbonate, 3ω (•), TMDSC (▲ ▽). The solid line through (• ▲ ▽) represents a VFTH-fit with the parameters $A = 13 \pm 1$, $B = (-700 \pm 100)$K and $T_\infty = (370 \pm 4)$K. The results of dielectric and mechanical measurements are indicated with ε'' and J'', respectively.

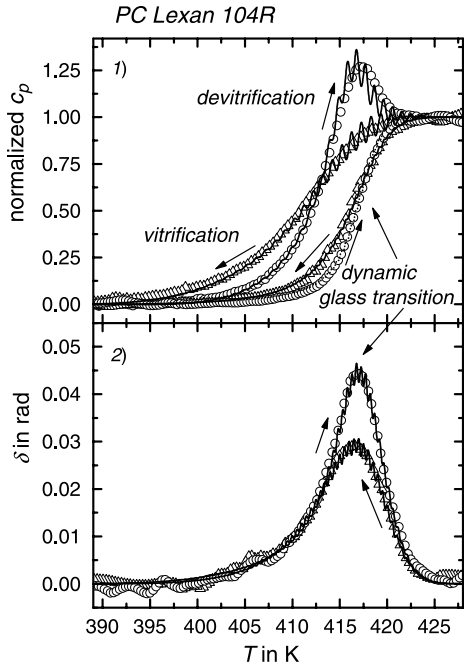

Fig. 2. Reduced heat capacity and phase angle from TMDSC measurements of bisphenol A-polycarbonate ($t_p = 60$ s, $A_T = 0.5$ K, $q_0 = \pm 1$ K/min). △, TMDSC on cooling; ○, TMDSC on heating; lines, TNM-model. Material constants and TNM-parameters: $C_{pl} = 1.6$ J/g K, $C_{pg} = 1.35$ J/g K, $\ln(\tau_0/s) = -31.12$, $\Delta h^*/R = 1580$ K, $T_\infty = 370$ K, $x = 0.24$, $\beta = 0.49$.

used to find the most suitable values to describe the standard DSC traces. The curves shown in Fig. 2 are obtained with $x = 0.24$, $\beta = 0.49$ and the other parameters derived from the VFTH-fit. As for polystyrene ($x = 0.22$ and $\beta = 0.56$ [33]) not only the calculated DSC traces but also the modulus of complex heat capacity and the phase angle between heat flow rate and heating rate agree very well with the measured curves. To check the applicability of the extended TNM-model under different experimental conditions all further calculations were performed with this single set of parameters. For bisphenol A-polycarbonate the agreement between the measured and the calculated heat capacities as well as the phase angles, δ_s, is even better than for polystyrene. In contrast to polystyrene there is no significant difference between measured and calculated $C_{p\ total}$ just below the glass transition on heating [33].

The influence of temperature scanning on complex heat capacity can be seen in the modulus of complex heat capacity but much more pronounced in the phase angle. Obviously the curves are reproduced by the TNM-model but the question remains what is the origin of these significant differences between heating and cooling. Similar results were obtained for polystyrene [33] where the influence of different cooling rates was seen too. The possible violation of the condition of stationarity and linearity [56] must be considered here.

Next, the influence of different cooling rates was studied for PC, see Fig. 3. At high cooling rates, 1 and 0.6 K/min, vitrification interferes with the dynamic glass transition. Because of the larger free volume in these samples compared to the sample cooled at 0.001 K/min a larger modulus of

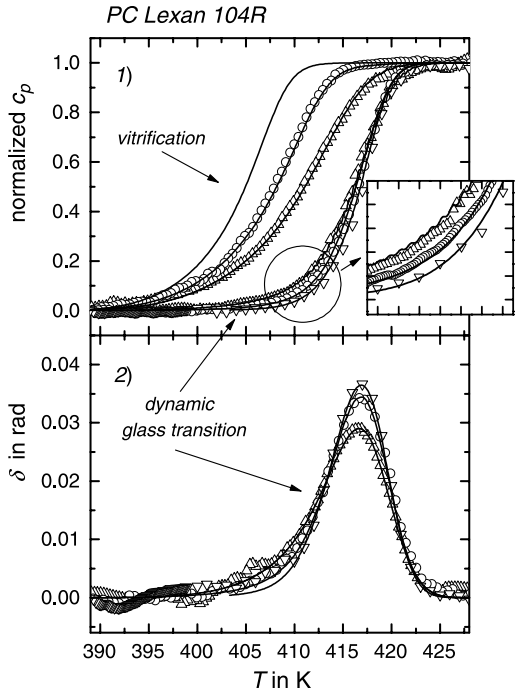

Fig. 3. Total heat capacity, modulus of complex heat capacity and phase angle between heat flow rate and heating rate for PC. The points represent TMDSC measurements and the lines TNM model calculations. $t_p=60$ s, $A_T=0.5$ K, and different underlying cooling rates △—$q_0=-1$ K/min; ○—$q_0=-0.05$ K/min; ▽—$q_0=-0.001$ K/min. All curves are smoothed over one period of the modulation.

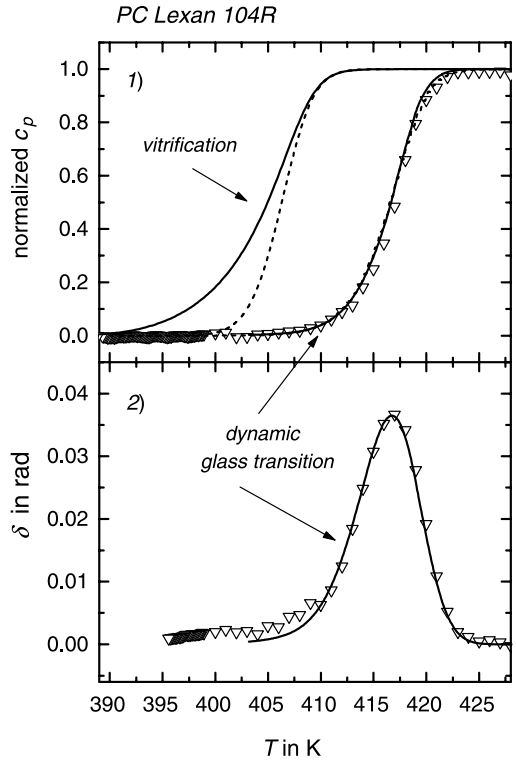

Fig. 4. Total heat capacity, modulus of complex heat capacity and phase angle between heat flow rate and heating rate for PC. The points represent TMDSC measurements and the lines TNM model calculations. $t_p=60$ s, $A_T=0.5$ K, $q_0=-0.001$ K/min, $x=0.24$—solid lines, and $x=1$—dashed lines. The solid and the dashed curves lie undistinguishable on top of each other for complex heat capacity and phase angle. All curves are smoothed over one period of the modulation.

complex heat capacity is measured at the low temperature edge of the dynamic glass transition. The measured phase angle shows also some cooling rate dependency because of the violation of stationarity at high scanning rates. This will be discussed in more detail in the next part of this paper. It should be mentioned that the extended TNM-model applied here is capable to describe all these features of the measured heat capacities correctly by a single set of parameters. Contrary to other modifications of the TNM here we were not interested in an improvement of the predictive power of the model for samples deep in the glassy state. All our experiments and modeling is limited to the temperature range near glass transition.

3.2. Interference between vitrification and dynamic glass transition

As long as vitrification and dynamic glass transition interfere, the acceleration of the relaxation because of the deviation from the equilibrium must be considered for the dynamic glass transition too. In the TNM-model this is done by the non-linearity parameter x which controls the contributions of actual and fictive temperature, respectively. In case of well separated vitrification and dynamic glass transition, in our case at cooling rate 0.001 K/min, the dynamic glass transition can be considered as an equilibrium relaxation process [26,30,42,54]. If this is true there should be no need to deal with the non-linearity parameter of the TNM-model under these particular conditions. Because there is a controversy about this, see e.g. Ref. [24], we have performed model calculations to check the influence of x under these conditions. Setting $x=1$ yields model curves without any contribution from T_f to the relaxation time. That means there is no influence of the non-equilibrium on the relaxation time as it is necessary to describe vitrification and devitrification, see total heat capacity in Fig. 3. Considering the dynamic glass transition as an equilibrium relaxation process means that there is no difference between T_f and T ($x=1$) above vitrification. In Fig. 4 the results are shown.

Obviously, no difference for the complex heat capacity at cooling rate 0.001 K/min can be seen for the model calculation with $x=0.24$ and $x=1$ and both are in agreement with the measured curves. Consequently, the dynamic glass transition can be considered as an equilibrium relaxation process. For the description of complex heat capacity in equilibrium, not superimposed with vitrification, it is sufficient to take into account the distribution of the relaxation times by means of a stretched exponential, parameter $\beta=0.49$, and their temperature dependence by means of a VFTH equation with the parameters $A=13\pm1$, $B=(-700\pm100)$K and $T_\infty=(370\pm4)$ K as determined by heat capacity spectroscopy. There is no need to distinguish between temperature and fictive temperature because there is no vitrification under these conditions, even not for the cooling part of the temperature oscillation, at the dynamic glass transition. At the thermal glass transition

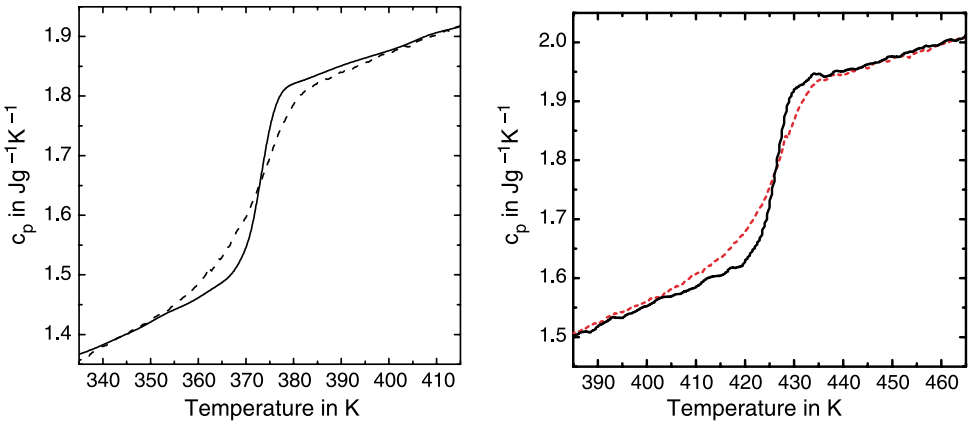

Fig. 5. Modulus of complex specific heat capacity from TMDSC (Setaram DSC 121; $t_p = 600$ s; $T_a = 0.25$ K)—full line and conventional DSC on cooling (Perkin–Elmer DSC-7; $q_0 = -10$ K/min)—dashed line, with approximately the same glass transition temperature for PS—left [60] and PEK—right [39].

(vitrification) at lower temperature there is of course a difference between both calculations because fictive temperature becomes significant different from temperature as soon as vitrification starts.

There is another argument that the system does not fall out of equilibrium during the cooling part of the temperature oscillation. If the system would fall out of equilibrium at local cooling during the course of the temperature modulation one would expect significant changes of the 'local vitrification' temperature by changing the temperature amplitude at constant frequency. This is because local cooling rate is proportional to temperature amplitude. If vitrification and devitrification would occur, the response would become strongly non-linear. But the calorimetric response at the dynamic glass transition of polystyrene is linear up to temperature amplitudes of 6 K as shown in Ref. [56]. This finding also supports the description of complex heat capacity as entropy compliance within the fluctuation dissipation theorem as discussed, e.g. in Refs. [42,54].

3.3. Relation between cooling rate and frequency

For several reasons it is of interest to know the corresponding molecular time scale for vitrification at linear cooling at rate q_0. It may be, as an example, of interest to include T_g values from calorimetric scan experiments in an Arrhenius diagram from dielectric or shear spectroscopy. Because TMDSC allows studying vitrification and dynamic glass transition simultaneously in an overlapping temperature range a direct comparison of the cooling rate and frequency dependence of glass transition is possible [23,24–40,55]. The most probable relaxation time τ for the dynamic glass transition, maximum of $c_p''(T)$, is directly available from $\omega\tau = 1$, where $\omega = 2\pi/t_p$ is the angular frequency of the temperature perturbation. In a next step the cooling rate can be determined which yields the same glass transition (vitrification) temperature. Here the fictive temperature is considered as the vitrification temperature [57–59]. Relation (1) derived from the fluctuation approach to glass transition was this way confirmed experimentally. For the constant a in Eq. (1) a value of 6 ± 3 was found for a wide variety of glass forming systems [39] in good agreement with the theoretical value 5.5 ± 0.1 [42]. To avoid any speculations concerning different models used to describe the behavior we have performed a direct comparison of experimental curves of vitrification and dynamic glass transition [39]. In Fig. 5 the results for polystyrene (PS) and a polyetherkethone (PEK) are shown.

For cooling curves the temperature of the half step is very close to the fictive temperature. As shown in Fig. 5 linear cooling at 10 K/min and TMDSC measurements at frequency 1.7 mHz yield approximately the same glass transition temperatures for PS and PEK. A comparison of truly experimental data for cooling rate and frequency dependence for a wide selection of different glass former was presented in Ref. [39]. Next, we make use of the extended TNM model to discuss the frequency and cooling rate dependence of dynamic glass transition and vitrification for bisphenol A-polycarbonate (PC) as we have done previously for PS in Ref. [33].

The frequency dependence of the dynamic glass transition for both measured and calculated points is obviously well described by the VFTH-curve which was derived from the measured points in a wider frequency range, see Fig. 1, and used for the model calculations. The cooling rate dependence of vitrification can, as discussed in Ref. [33], also be described by a VFTH-curve with the same temperature asymptote T_∞ but vertically shifted. In case of PC the shift equals $\log Y = 1.6$, see Fig. 7. Again the experimental results are well described by the TNM-model calculations. Hutchinson et al. [23] have published the results of similar calculations and experiments using the same PC sample. They got a shift of $\log Y = 0.59$ [23,37] which significantly differ from our value. To find the reason for this difference we applied Hutchinson's and our data treatment algorithms to the same set of data from the TNM model calculations. Hutchinson et al. [23,37] have defined the characteristic temperature of vitrification and dynamic glass transition as the temperature at which heat capacity reaches $\Delta c_p - \Delta c_p/e$, where $e = 2.718$ (Euler's number). In case of the normalized representation of the heat capacity data, $\Delta c_p = 1$, this equals 0.63. The corresponding values are indicated in Fig. 6. In contrast, we use the fictive temperature [57–59] to

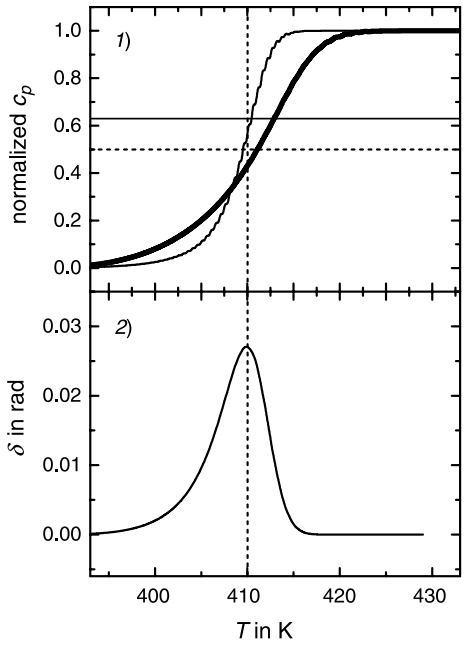

Fig. 6. Determination of the characteristic temperatures for dynamic glass transition and vitrification according to Hutchinson et al. [23,37] (solid horizontal line) and this work (dashed lines) on the example of model curves for PC. Thick curve—vitrification at cooling rate −1 K/min; Thin curves—modulus of complex heat capacity and phase shift at frequency 67 μHz (t_p = 15000 s).

characterize vitrification and the maximum of the imaginary part of complex heat capacity which equals the maximum of the phase angle to characterize the dynamic glass transition temperature, see Fig. 6.

Because the dynamic glass transition is narrow in temperature and the slope of the $c_p(T)$ curve is relatively steep the characteristic temperature according to Hutchinson et al. is only little higher than the maximum of the phase angle which coincides with the half step of the $c_p(T)$ increase. Vitrification results in a much broader transition region because of the influence of the structure (non-equilibrium) on the process. This broader transition region, consequently, yields a significant difference between the characteristic temperature according to Hutchinson et al. [23,37] and the fictive temperature which is commonly used as glass transition temperature. In Fig. 7 Hutchinson's et al. and our characteristic temperatures for one single set of model curves are shown as a function of frequency and cooling rate, respectively.

While the frequency dependencies are close to each other the cooling rate dependent points are different. The shift factors between the frequency and the cooling rate dependencies for both evaluations yield, as expected, the earlier published values, namely 0.69 for the evaluation according to Hutchinson et al. [23,37] and 1.6 according to Hensel et al. [39]. The controversy about the data as stated in Refs. [23,37] is therefore due to the different definitions of the characteristic temperatures by Hutchinson et al. and us, i.e. different degrees of vitrification are used as reference states for the determination of a. Why the comparison of the half step values as discussed by Hutchinson et al. in Ref. [23] also show some discrepancies

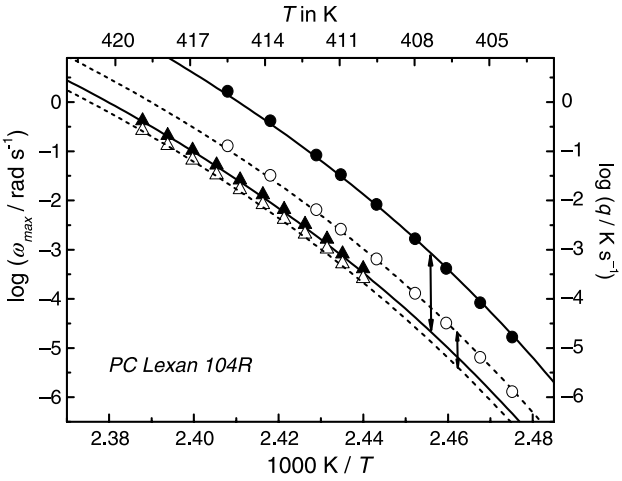

Fig. 7. Frequency (triangles) and cooling rate (circle) dependences of the characteristic temperatures of dynamic glass transition and vitrification, respectively, for model calculations for bisphenol A-polycarbonate. Open symbols—data treatments according to Hutchinson et al. [23,37]. Solid symbols—this study. The lines represent VFTH-fits to the data and the vertical arrows the shift factors log Y.

with our data can not be clarified because no experimental data for direct comparison are given in Ref. [23]. But as shown above our model calculation agree well with the measured data and both are in agreement with our previously published data for the logarithmic shift factor or $a\,\delta T$. The remaining difference between the models is the Arrhenius like dependence of the mean relaxation time used by Hutchinson et al. while in our calculations a VFTH dependence is taken into account. In our studies we took care to separate vitrification and dynamic glass transition at least at T_g and above. Sufficiently low cooling rates were always used.

4. Conclusion

The TNM-model extended by a non-Arrhenius temperature dependence of the relaxation time describes the features of the heat capacities measured in TMDSC scan experiments in the glass transition range of polystyrene [33] and polycarbonate reasonable well. A single set of parameters for each material is sufficient to describe total as well as complex heat capacity. This includes the curve shape, the frequency dependence of $T_g(\omega)$, the cooling rate dependence of $T_g(q_0)$ and possible interference between vitrification and dynamic glass transition. The parameters of the VFTH-equation, to describe the temperature dependence of the relaxation time, τ, are independently determined from heat capacity spectroscopy in a wide frequency range and not determined, as common for several studies, by curve fitting of the measured heat capacity. Consequently, only the stretched exponential parameter β and the non-linearity parameter x in the TNM-model have to be determined by a fitting procedure here.

Complex heat capacity at temperatures above vitrification can be considered as an equilibrium quantity. If temperature is scanned, contributions due to non-stationarity and non-linearity must be considered. These contributions are mainly

because of the strong temperature dependence of heat capacity in the glass transition range. This will be discussed in more detail in the next part of this paper.

The ratio between frequency and cooling rate, experimentally determined previously [39], is confirmed by experiment and model calculations under the condition that dynamic glass transition and vitrification are sufficiently separated by using slow cooling rates. The relation, Eq. (1), derived from Donth's fluctuation approach to glass transition [41,42] holds under the condition that fictive temperature is taken as the vitrification temperature and the maximum of the imaginary part of complex heat capacity as the dynamic glass transition. If other definitions are used, as in the case of Hutchinson's paper [23], the relation will change. The relation between cooling rate and frequency depends obviously on the degree of vitrification considered. For the correct description of the relation between scanning rate and frequency the non-Arrhenius temperature dependence of the relaxation time is essential.

Acknowledgements

We acknowledge valuable discussions with E. Donth, Halle, and J. Hutchinson (Aberdeen) and J. Hutchinson for providing the PC sample. This work was supported in part (S.W.) by the government of Mecklenburg-Vorpommern.

References

[1] Hodge IM. J Non-Cryst Sol 1994;169:211–66.
[2] Hutchinson JM. Prog Polym Sci 1995;20:703–60.
[3] Alvesa NM, Gomez Ribelles JL, Mano JF. Polymer 2005;46:491–504.
[4] Drozdov AD. Phys Lett A 1999;258:158–70.
[5] Avramov I, Gutzov I. J Non-Cryst Sol 2002;298:67–75.
[6] Lubchenko V, Wolynes PG. J Chem Phys 2004;121:2852–65.
[7] Scherer GW. J Am Ceram Soc 1984;67:504–11.
[8] Hodge IM. Macromolecules 1987;20:2897–908.
[9] Hutchinson JM, Montserrat S, Calventus Y, Cortes P. Macromolecules 2000;33:5252–62.
[10] Andreozzi L, Faetti M, Giordano M, Palazzuoli D, Zulli F. Macromolecules 2003;36:7379–87.
[11] Meseguer Duenas JM, Garayo AV, Romero Colomer F, Estelles JM, Gomez Ribelles JL, Monleon Pradas M. J Polym Sci, Part B: Polym Phys 1997;35:2201–17.
[12] Gomez Ribelles JL, Monleon Pradas M. Macromolecules 1995;28:5867–77.
[13] Gomez Ribelles JL, Monleon Pradas M, Garayo AV, Romero Colomer F, Estelles JM, Meseguer Duenas JM. Polymer 1997;38:963–9.
[14] Andreozzia L, Faetti M, Zulli F, Giordano M. Eur Phys J B 2004;41:383–93.
[15] Efremov MYu, Warren JT, Olson EA, Zhang M, Kwan AT, Allen LH. Macromolecules 2002;35:1481.
[16] Martin SW, Walleser J, Karthikeyan A, Sordelet D. J Non-Cryst Sol 2004;349:347–54.
[17] Andreozzi L, Faetti M, Giordano M, Zulli F. Macromolecules 2005;38:6056–67.
[18] Andreozzi L, Faetti M, Giordano M, Palazzuoli D. J Non-Cryst Sol 2003;332:229–41.
[19] Faetti M, Zulli F, Giordano M, Andreozzi L. Macromolecules 2004;37:8010–6.
[20] Hutchinson JM, Montserrat S. Thermochim Acta 1996;286:263–96.
[21] Hutchinson JM, Montserrat S. J Therm Anal 1996;47:103–15.
[22] Hutchinson JM, Montserrat S. Thermochim Acta 1997;305:257–65.
[23] Hutchinson JM, Montserrat S. Thermochim Acta 2001;377:63–84.
[24] Simon SL, McKenna GB. J Chem Phys 1997;107:8678–85.
[25] Simon SL, McKenna GB. Thermochim Acta 1997;307:1–10.
[26] Schawe JEK. Colloid Polym Sci 1998;276:565–9.
[27] Jiang Z, Hutchinson JM, Imrie CT. Polym Int 1998;47:72–5.
[28] Flikkema E, Vanekenstein GA, ten Brinke G. Macromolecules 1998;31:892–8.
[29] Simon SL, McKenna GB. Thermochim Acta 2000;348:77–89.
[30] Moon IK, Jeong YH. Thermochim Acta 2001;377:51–61.
[31] Schawe JEK. J Polym Sci, Part B: Polym Phys 1998;36:2165–75.
[32] Salmeron M, Torregrosa C, Vidaurre A, Meseguer Duenas JM, Pradas MM, Ribelles JL. Colloid Polym Sci 1999;277:1033–40.
[33] Weyer S, Merzlyakov M, Schick C. Thermochim Acta 2001;377:85–96.
[34] Scherer GW. J Am Ceram Soc 1984;67:504–11.
[35] Hodge IM. Macromolecules 1987;20:2897–908.
[36] Hempel E, Kahle S, Unger R, Donth E. Thermochim Acta 1999;329:97–108.
[37] Jiang Z. PhD Thesis. UK: University of Aberdeen; 2000.
[38] Schawe JEK. J Therm Anal 1996;47:475–84.
[39] Schick C, Hensel A. J Non-Cryst Sol 1998;235–237:510–6.
[40] Donth E, Korus J, Hempel E, Beiner M. Thermochim Acta 1997;305:239–49.
[41] Donth E. Relaxation and thermodynamics in polymers, glass transition. Berlin: Akademie Verlag; 1992.
[42] Donth E. The glass transition: relaxation dynamics in liquids and disordered materials. Berlin: Springer; 2001.
[43] Gobrecht H, Hamann K, Willers G. J Phys E: Sci Instrum 1971;4:21–3.
[44] Reading M. Trends Polym Sci 1993;8:248–53.
[45] Wunderlich B, Jin YM, Boller A. Thermochim Acta 1994;238:277–93.
[46] Schawe JEK. Thermochim Acta 1995;260:1–16.
[47] Schawe JEK. Thermochim Acta 1995;261:183–94.
[48] Schawe JEK, Hohne GWH. Thermochim Acta 1996;287:213–23.
[49] Sarge SM, Hemminger W, Gmelin E, Hohne GWH, Cammenga HK, Eysel W. J Therm Anal 1997;49:1125–34.
[50] Hensel A, Schick C. Thermochim Acta 1997;305:229–37.
[51] Schick C, Jonsson U, Vassilev T, Minakov A, Schawe J, Scherrenberg R, et al. Thermochim Acta 2000;347:53–61.
[52] Weyer S, Hensel A, Schick C. Thermochim Acta 1997;305:267–75.
[53] Weyer S. Beschreibung des Einfrierens und der komplexen Wärmekapazität am Glasübergang mit einem erweiterten TNM-Modell. PhD Thesis. Germany:University of Rostock; 2002.
[54] Birge NO, Nagel SR. Phys Rev Lett 1985;54:2674–7.
[55] Hensel A, Dobbertin J, Schawe JEK, Boller A, Schick C. J Therm Anal 1996;46:935–54.
[56] Schick C, Merzlyakov M, Hensel A. J Chem Phys 1999;111:2695–700.
[57] Tool AQ. J Am Ceram Soc 1946;29:240–53.
[58] Richardson MJ, Savill NG. Polymer 1975;16:753–7.
[59] Moynihan CT, Easteal AJ, De Bolt MA, Tucker J. J Am Ceram Soc 1976;59:12–16.
[60] Weyer S, Hensel A, Korus J, Donth E, Schick C. Thermochim Acta 1997;305:251–5.